Polymer 43 (2002) 2501–2506

polymer

www.elsevier.com/locate/polymer

Effects of coupling agent and morphology on the impact strength of high density polyethylene/$CaCO_3$ composites

Z.H. Liu[a], K.W. Kwok[a,*], R.K.Y. Li[b], C.L. Choy[a]

[a]Department of Applied Physics and Materials Research Centre, The Hong Kong Polytechnic University, Hung Hom, Kowloon, Hong Kong, China
[b]Department of Physics and Materials Science, City University of Hong Kong, Tat Chee Avenue, Kowloon, Hong Kong, China

Received 1 August 2001; received in revised form 13 November 2001; accepted 21 November 2001

Abstract

The effects of coupling agent, particle diameter (*d*), particle volume fraction (V_c), particle size distribution and average matrix ligament thickness ($\bar{T}$) on the impact strength of high density polyethylene (HDPE)/$CaCO_3$ composites have been investigated. A coupling agent is required for dispersing the $CaCO_3$ particles ($d \sim 0.6$–5.6 μm) without agglomeration in the HDPE matrix. The optimum weight ratio of coupling agent to $CaCO_3$ particles for achieving the highest toughening efficiency is about 0.05, which is independent of *d*, V_c and size distribution of $CaCO_3$ particles. HDPE/$CaCO_3$ composites undergo a brittle–ductile transition in the range $V_c = 0.1$–0.3, and the maximum impact strength achieved depends on *d* and size distribution. Above the transition, the impact strength of the composite decreases with increasing V_c. In general, a HDPE/$CaCO_3$ composite with smaller *d* and broader size distribution has a higher toughness. A single brittle–ductile transition curve is not obtained when the impact strength is plotted against $\bar{T}$. Shear yielding of the polymer matrix induced by debonding at the interface between $CaCO_3$ and HDPE is shown to be the major toughening mechanism. © 2002 Elsevier Science Ltd. All rights reserved.

Keywords: Impact strength; Morphology; HDPE/$CaCO_3$ composites

1. Introduction

Polymer toughening is usually achieved by the incorporation of rubber particles in a polymer matrix [1–7]. The fracture toughness of rubber-modified polymers is mainly determined by morphological factors, including particle size, particle volume fraction, particle size distribution and particle spatial distribution [1–9]. Most of the previous works show that the combined effects of various morphological factors can be described by a single parameter, the matrix ligament thickness *T* (surface-to-surface interparticle distance), and a single brittle–ductile transition curve is obtained when the impact strength is plotted against *T*. When *T* is smaller than a critical value T_c, matrix shear yielding occurs and the material becomes very tough. However, Liu et al. found that different brittle–ductile transition curves were obtained for poly(vinyl chloride) (PVC)/nitrile rubber (NBR) blends with different particle spatial distributions [10]. They demonstrated that the toughening efficiency in the blend with rubber particles dispersed in pseudo-network form was higher than that in the blend with uniformly dispersed rubber particles. Although rubber-modified polymers have very high fracture toughness, they suffer from the drawback of having low stiffness. On the other hand, the stiffness of a polymer can be enhanced substantially by incorporating rigid particles [11]. However, the toughness of the material usually decreases.

Recently, it has been found that simultaneous enhancement of toughness and stiffness can be achieved in a polymer/rigid particle system, e.g. PVC/$CaCO_3$ [12] and high density polyethylene (HDPE)/$CaCO_3$ [13,14]. Fu et al. [13] and Bartczak et al. [14] showed that the toughness of HDPE/$CaCO_3$ composites increased dramatically when the matrix ligament thickness *T* was smaller than T_c. They concluded that debonding at the interface between $CaCO_3$ and HDPE induced shear yielding in the matrix, hence a considerable amount of impact energy was absorbed during the fracture process. A single brittle–ductile transition curve was not obtained for HDPE/$CaCO_3$ composites. The impact strength of toughened HDPE/$CaCO_3$ composites depended not only on *T*, but also on the diameter of $CaCO_3$ particles. In addition, the toughness of HDPE/$CaCO_3$ composites decreased as *T* decreased below T_c [14]. Bartczak et al. [14] suggested that the decrease in toughness was caused by the agglomeration of $CaCO_3$ particles. Similar behavior

---

* Corresponding author: Tel.: +852-2766-5667; fax: +852-2333-7629.
E-mail address: apkwkwok@polyu.edu.hk (K.W. Kwok).

0032-3861/02/$ - see front matter
PII: S0032-3861(02)00048-4

was observed in polypropylene/$CaCO_3$ composites by Jancar et al. [15]. However, they attributed the decrease in toughness to the decrease in matrix effective cross section instead.

To incorporate a mineral filler into a polymer, coupling agents are usually used in order to improve the dispersion of the filler. Coupling agents at fixed weight ratios have been used in previous works on HDPE/$CaCO_3$ composites [13,14]. However, the effect of coupling agent at different weight ratios has not been studied. In the present work, the effect of coupling agent on the impact strength of HDPE/$CaCO_3$ composites has been investigated. The effects of particle diameter, volume fraction and size distribution of $CaCO_3$ particles have also been discussed.

2. Experimental

2.1. Sample preparation

The polymer used in this work was high-density polyethylene (HDPE) Hi-zex® 7000F supplied by Mitsui Petrochemical Industrials, Ltd. Five types of $CaCO_3$ particles of various sizes were used as fillers; they were abbreviated as Q1, Q2, Q3 (supplied by J.M. Huber Corporation) and S1 and S2 (supplied by Sichuan Hualian Medicine Industry Co. Ltd, China). The coupling agent, isopropyltriisostearoyl titanate, was supplied by Jiangshu Changzhou Lijing Chemicals Ltd, China.

The $CaCO_3$ particles were first heated in an oven at 140 °C for 6 h to remove the moisture, and then mixed with various amounts of the coupling agent immediately in a high-speed mixer for 15 min. The weight ratio w_a of coupling agent to $CaCO_3$ particles ranged from 0 to 0.1. The treated particles were finally blended with HDPE in a Brabender mixer at 140 °C for 15 min. After blending, the materials were compression-molded at 150 °C into flat plates, from which impact test specimens of dimensions 70 mm × 12.4 mm × 4 mm were cut. A notch of depth 2.5 mm and angle 45° was made at the middle of each specimen. The radius of curvature at the apex of the notch was 0.25 mm. The volume fraction of $CaCO_3$ particles V_c was calculated using the weight fraction of $CaCO_3$ particles and the densities of HDPE (0.96 g/cm^3) and $CaCO_3$ (2.7 g/cm^3).

2.2. Property measurements

The Izod impact strength was measured on notched specimens using a Ceast impact tester according to ASTM D-256. The impact speed was 3.46 m/s. All the measurements were performed at room temperature and five specimens were tested for each composite.

Micrographs of the fracture surfaces of composite specimens were taken by using a scanning electron microscope (Leica Stereoscan 440). Generally, the $CaCO_3$ particles have an irregular shape, so the equivalent diameter of the particles was determined using commercial software, Optimas® 5. For each composite specimen, the sizes of about 400 particles on the fracture surface were measured. From these data the average particle diameter d and particle size distribution parameter σ (to be defined) were calculated.

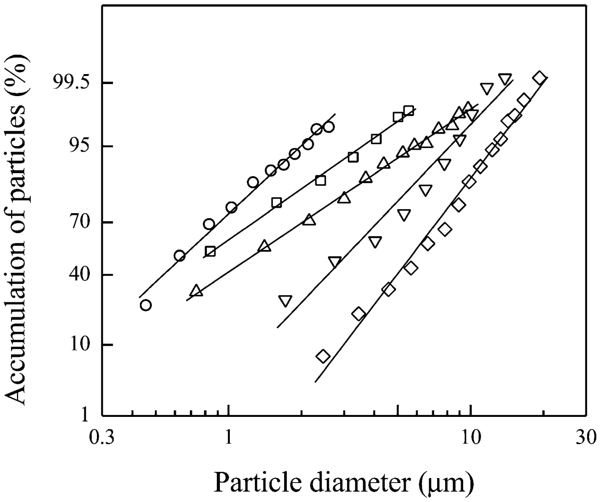

Fig. 1. Cumulative particle size distribution of the $CaCO_3$ particles in composite specimens. ○, □, △, ▽ and ◇ denote the data for Q1, Q2, Q3, S1 and S2, respectively.

3. Results and discussion

3.1. Size and size distributions of $CaCO_3$ particles

The cumulative number (in %) of $CaCO_3$ particles versus the particle diameter is shown in Fig. 1. It is seen that the size distributions of all the particles fit the log-normal distribution. The corresponding average particle diameter d, defined as the diameter at 50% cumulative number of $CaCO_3$ particles, and the size distribution parameter σ, defined as the ratio of the particle diameter at 84% cumulative number of $CaCO_3$ particles to that at 50%, are obtained from the graph [8]. The minimum value of $\sigma = 1$ corresponds to a uniform size distribution; a larger σ value implies a broader distribution. As seen from Table 1, the observed average diameters of Q1, Q2, Q3, S1 and S2 are 0.6, 0.8, 1.2, 3.0, and 5.6 μm, respectively, and the size distribution of the particles is quite broad ($\sigma \sim 1.66$–2.62).

Table 1
Average diameter (d) and size distribution parameters (σ) of the $CaCO_3$ particles used in this work

$CaCO_3$ particle	d (μm)	σ
Q1	0.6	1.99
Q2	0.8	2.51
Q3	1.2	2.62
S1	3.0	1.87
S2	5.6	1.66

3.2. Effect of coupling agent

It is difficult to disperse the $CaCO_3$ particles uniformly in a HDPE matrix without using the coupling agent, so results for the composites without coupling agent will not be presented in this work. A very small amount of the coupling agent (weight ratio of coupling agent to $CaCO_3$ particles $w_a = 0.025$) is sufficient for dispersing the $CaCO_3$ particles. The spatial distribution of $CaCO_3$ particles on the fracture surface of the HDPE/Q1 composite ($d = 0.6$ μm, $V_c = 0.19$, and $w_a = 0.025$) is shown in Fig. 2. It is seen that the $CaCO_3$ particles are quite uniformly dispersed in the composite and no severe agglomeration is observed. Similar spatial distribution has been observed in the other composites with various V_c and $w_a \leq 0.05$. However, aggregates of $CaCO_3$ particles, as verified by energy dispersive X-ray (EDX) analysis in a scanning electron microscope, are found in the composites with $w_a > 0.05$. Fig. 3 shows, as an example, the aggregates of $CaCO_3$ particles found on the fracture surface of the HDPE/Q1 composite with $w_a = 0.075$, and the EDX spectrum of the aggregates is shown in Fig. 4. The number of aggregates increases with increasing w_a. This is probably because if too much coupling agent is used, the excess coupling agent will cause the $CaCO_3$ particles to stick together to form aggregates during the pre-mixing process.

The dependence of the notched Izod impact strength on V_c for HDPE/Q1 composites with various w_a is shown in Fig. 5. It can be seen that all the composites undergo a brittle–ductile transition. The impact strength of the composites increases with increasing V_c and reaches a maximum value at $V_c = V_o$ ($\sim$0.2). V_o is defined as the optimum value of V_c for toughening, i.e. the V_c value at which the impact strength is maximum. As V_c increases above V_o the impact strength decreases, and no toughening effect is observed at $V_c > 0.3$. It is also seen that the toughening efficiency depends on w_a. A small amount of coupling agent ($w_a = 0.025$) can give rise to a good dispersion of $CaCO_3$ particles and effective toughening of the composite. The impact strength of the HDPE/Q1 composite ($d = 0.6$ μm, $V_c = 0.19$, and $w_a = 0.025$) is more than twice as large as that of HDPE. Probably due to better dispersion of the particles, the toughening efficiency increases as w_a increases from 0.025 to 0.05. The HDPE/Q1 composite with $w_a = 0.05$ has a notched Izod impact strength of about 600 J/m, about three times larger than that of HDPE. However, at higher w_a, the toughening efficiency decreases with increasing w_a. This may be caused by the agglomeration of $CaCO_3$ particles (Fig. 3).

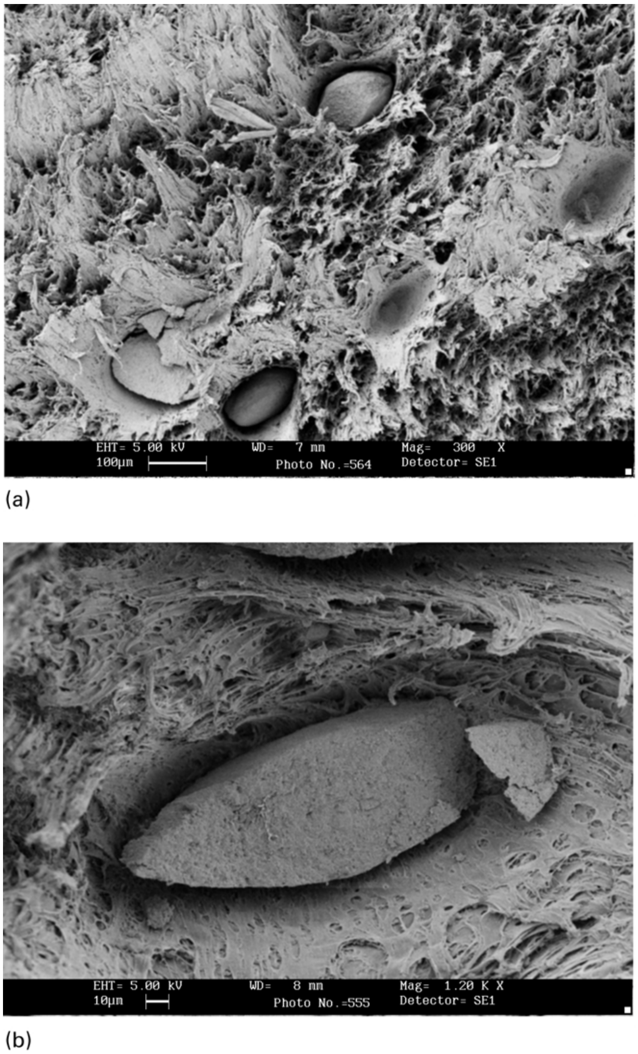

Fig. 3. SEM micrograph of the fracture surface of the HDPE/Q1 composite ($V_c = 0.19$, $w_a = 0.075$, and $d = 0.6$ μm) showing the agglomeration of $CaCO_3$ particles. (a) magnification = 300 ×; (b) magnification = 1200 ×.

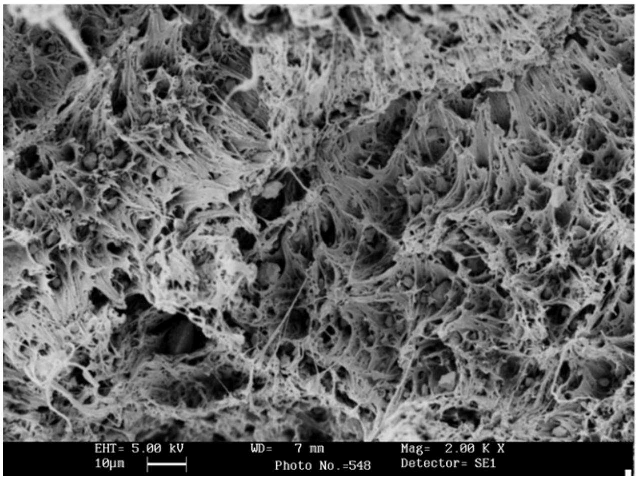

Fig. 2. SEM micrograph of the fracture surface of the HDPE/Q1 composite ($V_c = 0.19$, $w_a = 0.025$, and $d = 0.6$ μm) showing the spatial distribution of $CaCO_3$ particles.

Unlike HDPE/Q1 composites, HDPE/Q3 composites ($d = 1.2$ μm) are toughened only in the range of V_c from 0.2 to 0.4 (Fig. 6). The impact strength of the composites first decreases and then increases with increasing V_c, and reaches a maximum value at $V_c \sim 0.26$ (V_o). The effect of

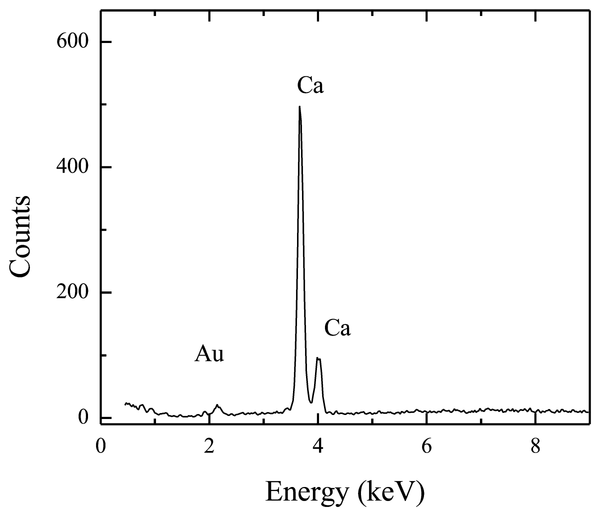

Fig. 4. EDX spectrum of an aggregate found on the fracture surface of the HDPE/Q1 composite ($V_c = 0.19$, $w_a = 0.075$, and $d = 0.6$ μm) indicating that the aggregate consists mainly of $CaCO_3$.

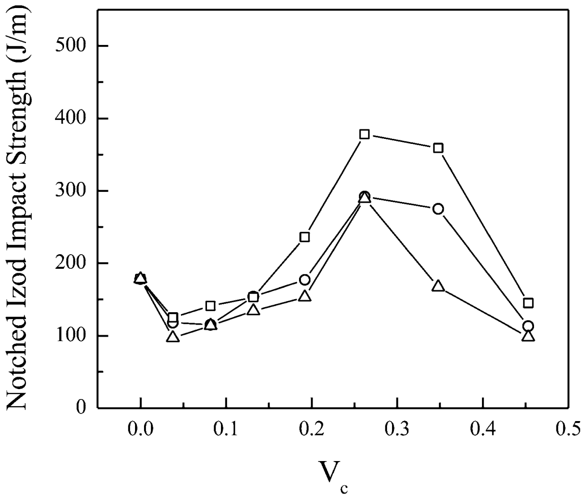

Fig. 6. Notched Izod impact strength of the HDPE/Q3 composites ($d = 1.2$ μm) as a function of volume fraction of $CaCO_3$ particles, V_c. Data: ○, $w_a = 0.025$; □, $w_a = 0.05$; △, $w_a = 0.075$.

w_a on the toughness is similar for both HDPE/Q1 and HDPE/Q3 composites. The impact strength of HDPE/Q3 composites also has the highest value at $w_a = 0.05$. Therefore, in the following section, we will concentrate on the composites with $w_a = 0.05$.

Extensive stress whitening has been observed near the fracture surface of the toughened composites ($V_c \leq V_o$). As an example, the fracture surface of a toughened HDPE/Q1 composite ($d = 0.6$ μm, $V_c = 0.19$, $w_a = 0.05$) is shown in Fig. 7. It is seen that $CaCO_3$ particles are detached from the polymer matrix and the matrix exhibits extensive plastic deformation. This is consistent with the proposed mechanism that debonding of $CaCO_3$ particles from the HDPE matrix induce shear yielding of the matrix, and hence give rise to extra dissipation of impact energy [5,6,13]. At $V_c > V_o$, there is less matrix shear yielding, and stress whitening only occurs on the fracture surface; the surface-to-surface interparticle distance (matrix ligament thickness) and the effective matrix cross-section are now very small, and the local constrain in the polymer matrix near the particles increases. As a result, cracks will propagate faster and the matrix beneath the fracture surface will be prohibited from deforming plastically. This leads to a decrease in the impact strength (Fig. 5) [15].

3.3. *Effect of morphological parameters on impact strength*

Fig. 8 shows the dependence of the impact strength on V_c for composites containing $CaCO_3$ particles of different

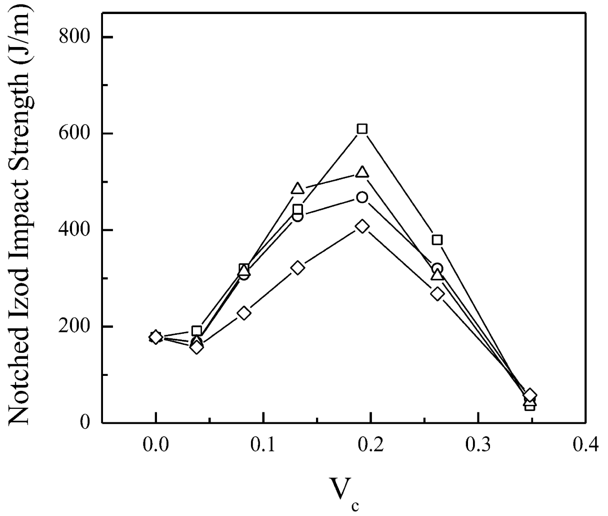

Fig. 5. Notched Izod impact strength of the HDPE/Q1 composites ($d = 0.6$ μm) as a function of volume fraction of $CaCO_3$ particles, V_c. Data: ○, $w_a = 0.025$; □, $w_a = 0.05$; △, $w_a = 0.075$; ◇, $w_a = 0.1$.

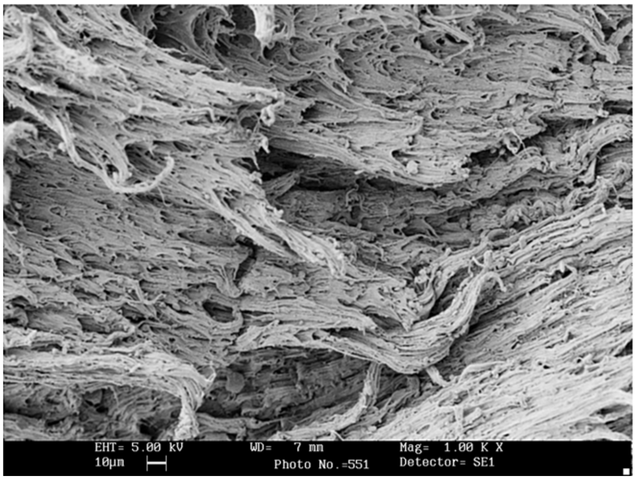

Fig. 7. SEM micrograph of the fracture surface of the HDPE/Q1 composite ($V_c = 0.19$, $w_a = 0.05$, and $d = 0.6$ μm) showing extensive plastic deformation of the matrix.

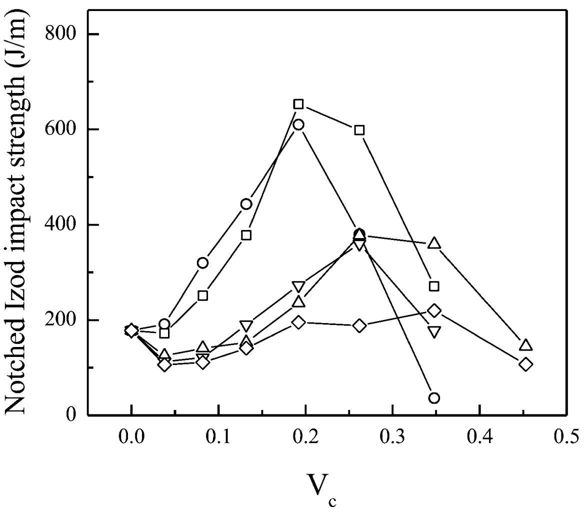

Fig. 8. Notched Izod impact strength of the HDPE/CaCO$_3$ composites as a function of volume fraction of CaCO$_3$ particles, V$_c$. Data: ○, $d = 0.6$ μm; □, $d = 0.8$ μm; △, $d = 1.2$ μm; ▽, $d = 3.0$ μm; ◇, $d = 5.6$ μm.

diameters. It is seen that the impact strengths of HDPE/Q1 ($d = 0.6$ μm) and HDPE/Q2 ($d = 0.8$ μm) composites show similar dependence on V_c. The impact strengths of these two composites are almost the same, and increase with increasing V_c when V_c is smaller than 0.2. At $V_c = V_o \sim 0.2$, their impact strengths reach a maximum value of about 600 J/m. At $V_c > V_o$, their impact strengths decrease with increasing V_c, and the impact strength of HDPE/Q1 is smaller than that of HDPE/Q2. This may be due to the narrower size distribution of Q1 (Table 1).

As shown in Fig. 8, the toughening efficiency in composites containing larger CaCO$_3$ particles (HDPE/Q3, $d = 1.2$ μm; HDPE/S1, $d = 3.0$ μm) is significantly lower, and no toughening effect is observed for composites with very large particles (HDPE/S2, $d = 5.6$ μm). It is interesting to note that HDPE/Q3 and HDPE/S1 composites exhibit similar variations of impact strength with V_c although Q3 is about three times smaller than S1. They have a maximum impact strength of about 380 J/m at $V_c = V_o \sim 0.26$. Probably due to the narrower size distribution of S1, the toughening efficiency in HDPE/S1 is lower at $V_c > V_o$. It can be seen that the impact strength of HDPE/CaCO$_3$ composites depends not only on the diameter and volume fraction of CaCO$_3$ particles, but also on the size distribution of the particles.

3.4. Brittle–ductile transition

Previous studies [1–4] have shown that the effects of particle size and volume fraction of rubber particles on the impact strength of rubber-modified polymers can be described by a single brittle–ductile transition curve in which the impact strength is plotted against the matrix ligament thickness *T*. However, in the calculation of *T*, it is assumed that the particles have the same diameter and are arranged in a cubic lattice. As mentioned in the previous section, the CaCO$_3$ particles used in this work have very broad size distribution ($\sigma \sim 1.66$–2.62) (Fig. 2), which has a great influence on *T*. To account for the size distribution of CaCO$_3$ particles, an average ligament thickness $\bar{T}$ is used [16]:

$$\bar{T} = d\left(\left(\frac{\pi}{6V_c}\right)^{\frac{1}{3}}\exp(1.5\ln^2\sigma) - \exp(0.5\ln^2\sigma)\right) \qquad (1)$$

where d is the average particle diameter, σ is the size distribution parameter for log-normal size distribution, and V_c is the volume fraction of particles. Fig. 9 shows the variation of the impact strength of HPDE/CaCO$_3$ composites with $\bar{T}$. Unlike rubber-modified polymers, a single brittle–ductile transition curve is not observed for HPDE/CaCO$_3$ composites. At high $\bar{T}$, the impact strengths of HDPE/Q2, HDPE/Q3 and HDPE/S1 composites are almost the same; they increase with decreasing $\bar{T}$, reaching different maximum values at different $\bar{T}$, and then decrease. As discussed in Section (3.2), when the matrix ligament thickness is very small, the matrix beneath the fracture surface will be prohibited from deforming plastically, thereby resulting in a decrease in the impact strength [15]. It is interesting to note that the impact strength of HDPE/Q1 has a similar $\bar{T}$ dependence as the other composites but the maximum occurs at a much lower $\bar{T}$ value. The separation of the transition curves may be due to the non-spherical shape of the CaCO$_3$ particles, thus making Eq. (1) invalid. In addition, the deviation of the spatial distribution of CaCO$_3$ particles from a cubic lattice may also lead to uncertainty in determining $\bar{T}$ [17].

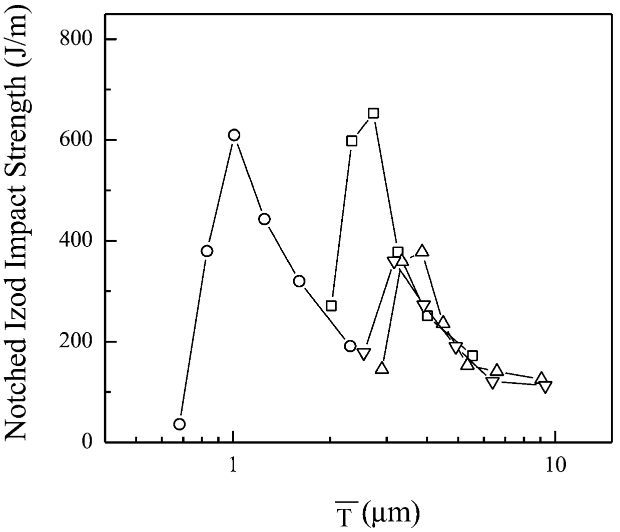

Fig. 9. Notched Izod impact strength of the HDPE/CaCO$_3$ composites as a function of average matrix ligament thickness, $\bar{T}$. Data: ○, $d = 0.6$ μm; □, $d = 0.8$ μm; △, $d = 1.2$ μm; ▽, $d = 3.0$ μm.

4. Conclusions

This study reveals that the notched Izod impact strength of HDPE can be improved significantly by the incorporation of rigid $CaCO_3$ particles. A coupling agent is needed for dispersing fine $CaCO_3$ particles ($d \sim 0.6$–$5.6\ \mu m$) without agglomeration in the HDPE matrix, and the content of the coupling agent affects the toughening efficiency. The optimum weight ratio of coupling agent to $CaCO_3$ particles for achieving the highest toughening efficiency is found to be about 0.05, which is independent of the particle diameter (d), volume fraction (V_c) and size distribution of $CaCO_3$ particles. On the other hand, the toughening efficiency in HDPE/$CaCO_3$ composites depends on d, V_c and size distribution. For HDPE/$CaCO_3$ composites with $d \leq 5.6\ \mu m$, a brittle–ductile transition occurs as V_c increases to V_o ($\sim$0.2–0.3), and the maximum impact strength achieved depends on d and size distribution. In general, a composite with smaller d and broader size distribution is tougher. Shear yielding of the polymer matrix induced by debonding at the interface between $CaCO_3$ and HDPE is shown to be the major energy absorption mechanism. At $V_c > V_o$, the impact strength of the composites decreases considerably. The polymer matrix is prohibited from shear yielding due to the increase of the local constraint in the polymer matrix near the particles. The combined effects of d, V_c and size distribution on the toughness of HDPE/$CaCO_3$ composites cannot be described by a single brittle–ductile transition curve of the impact strength versus the average matrix ligament thickness.

Acknowledgements

The financial support from the Hong Kong Polytechnic University Postdoctoral Fellowship Scheme and the Hong Kong Research Grant Council are acknowledged.

References

[1] Wu S. Polymer 1985;26:1855.
[2] Wu S. Polym Engng Sci 1990;30:753.
[3] Jancar J, DiAnselmo A, DiBenedetto AT. Polym Comm 1991;32:367.
[4] Li Q, Zheng WG, Qi ZN, Zhu XG, Choy CL. Science in China (B) 1993;36:18.
[5] Liu ZH, Zhang XD, Zhu XG, Li RKY, Qi ZN, Wang FS, Choy CL. Polymer 1998;39:5019.
[6] Bartczak Z, Argon AS, Cohen RE, Weinberg M. Polymer 1999;40:2331.
[7] Takaki A, Yasui H, Narisawa I. Polym Engng Sci 1997;37:105.
[8] Bucknall CB, Karpodinis A, Zhang XC. J Mater Sci 1994;29:3377.
[9] Sue HJ, Yee AF. Polym Engng Sci 1996;36:2320.
[10] Liu ZH, Zhang XD, Zhu XG, Li RKY, Qi ZN, Wang FS, Choy CL. Polymer 1998;39:5035.
[11] Meddad A, Fisa B. Appl Polym Sci 1997;64:653.
[12] Mathur KK, Driscoll SB. J Vinyl Technol 1982;4:81.
[13] Fu Q, Wang GH, Shen J. J Appl Polym Sci 1993;49:673.
[14] Bartczak Z, Argon AS, Cohen RE, Weinberg M. Polymer 1999;40:2347.
[15] Jancar J, DiBenedetto AT, DiAnselmo A. Polym Engng Sci 1993;33:559.
[16] Liu ZH, Zhang XD, Zhu XG, Qi ZN, Wang FS. Polymer 1997;38:5267.
[17] Liu ZH, Li RKY, Tjong SC, Qi ZN, Wang FS, Choy CL. Polymer 1998;39:4433.